Effect of the Leading-Edge Sweep on Wrap-Around Fins

K. MADHULAALASA*,[1], P. SHISHIR[1], P. Venkata Sai PRASAD[1],
P. K. MOHANTA[1], Swapnil SAPKALE[2]

*Corresponding author
[1]Department of Aeronautical Engineering,
Institute of Aeronautical Engineering, Dundigal,
Hyderabad-500 043, India,
janukurma00@gmail.com*, shishir.potineni@gmail.com,
saipunugu.2000@gmail.com, prasanta.mohanta@gmail.com
[2]Department of D&E, Bharat Dynamics Limited, Kanchanbagh,
Hyderabad-500 058, India,
segdne.bdl@bdl-india.in

DOI: 10.13111/2066-8201.2022.14.1.6

Received: 04 July 2021/ Accepted: 24 January 2022/ Published: March 2022

Abstract: *In this paper, the investigation was performed to determine the effect of leading-edge angle and leading-edge sweep on the aerodynamic coefficients of the projectile geometry and analyze the effect of roll moment on the fins at various operating conditions. A group of four models were considered, standard TTCP with the blunt leading edge and with 45° leading-edge along with modified TTCP with the blunt leading edge along with 30° sweep and with 45° leading-edge along with 30° sweep. The flow field solutions were obtained and considered as a function of roll moment coefficients, which are then compared to other numerical models and experimental results. The standard wrap-around TTCP models were subjected to varying velocities ranging from Mach 1.5 to 2.5. WAFs are considered a choice for spinning tube-launched projectiles because of their high packing factor and instant deployment. The computational grids have been built to accurately reflect the fin edge shape of the experimental model. The significant parameter of the WAF is the rolling moment, that was computed using CFD and compared with available experimental test data.*

Key Words: *Wrap-around fins, rolling moment, projectile, computational grid, fluid domain, TTCP*

1. INTRODUCTION

Missiles power is seen as the utmost strength of the countries in today's time, and the country that owns a more significant number of missiles and has state-of-the-art R&D will outperform others in the global race for supremacy. Currently, the USA, Russia, India, and China continue to remain the strongest in the world because of their missile strength. A Missile is a state-of-art unmanned rocket system fabricated to carry the payload to a designated point to destroy the target.

Missile control fins are arguably the most effective way of monitoring and steering a tactical missile to a target. They can efficiently produce the required maneuvering force in two ways, either by a direct effort near the center of gravity or through the rotation of the missile to a higher angle of attack. The primary consequences of control fins on the missile system configuration are usable maneuvering force and maneuvering reaction.

There have been many developments in fin configurations, and one of them is Wrap-around fins (WAF).

Wrap-around fins have been used on anti-tank rockets, cruise missiles, and other weapons for decades. Its ability to provide aerodynamic stabilizing attributes for free-flight systems significantly alleviated the missiles configuration constraints. Wrap-around fins are carved into the launch tube before launch, saving much place in the tube. It is also caved in the initial stages of the missile to reduce drag and can be extended when the situation of missile management arises. Dahlke [1] published a study on wrap-around fins in 1973, which was cited a plethora of times in other studies.

Several variables of wrap-around fins were taken into consideration during the measurement of the missiles with wrap-around fins in two wind tunnels; a transonic wind tunnel and a supersonic wind tunnel. Dahlke explained that missiles equipped with planar fins and wrap-around fins comprise equal static stability derivatives when working at zero angle of attack. They have a drag, which is 1.1 times that of a flat fin, which has an equal planform area. It is also found that missiles with wrap-around fins also induce roll moment at zero angle of attack in wind tunnel tests. [2] Besides that, as a function of Mach number, the trajectory of the self-implicated roll moment can be modified. The crossover happened when the flight speed was about Mach 1.0. The fin force administered apart from the centre of curvature determines the moment direction at supersonic speeds. In contrast, the force directed towards the centre determines the moment direction at subsonic speeds.

Arnan [3] et.al analysed the self-induced rolling moment of wrap-around fins. They used a numerical approach to solve the subsonic potential flow over the geometry with zero incidences. They concluded that at the zero angle of attack in a subsonic flow, the self-inflicted rolling moment of wrap-around-fins could be caused by the radial velocity portion produced on the fins by wake flow, using a non-linear vortex-lattice method.

In 1999, Seung-Kil Paek [4] et. al researched the wrap-around fins with Euler equations. By making use of 3-d Euler equations with time marching solutions, the wrap-around fins having flow field solutions of a projectile have been evaluated in a supersonic environment. As stated in the findings, the tip design and the edge shape have an essential impact on the roll moment of the wrap-around fin. Slobodan Mandic [5] used a wind tunnel to calculate the rolling moment coefficients with three fin configurations. Two versions had wrap-around fins, while the third had flat fins derived from the calculation of the wrap-around fins. There are limited amounts of numerical analysis on the roll characteristics of wrap-around fins. Solely the roll generating moment constant was determined for non-axisymmetric bodies using Navier-stokes and Euler computational codes. Projectile designers rely on approximate strategies to work out the roll damping moment constant or the steady-state roll rate.

Table 1: Brief review of previous experimental and computational work

Source of data	Model type	Type of analysis	Range of Mach Number	Roll reversal point
P. Seung-Kil Paek, et.al. [4]	Standard TTCP	Computational	1.5-2.5	1.8
H. L. Edge [6]	Standard TTCP	Computational and experimental	1.3-3.0	1.7
Y.K.Jung, et.al. [7]	TTCP standard configuration	Computational and compared with numerical study	1.6-2.2	~ 1.8
L. W. Brett [8]	WAF with angle of attack	Computational and experimental	1.5-3.0	-

M. Slobodan [5]	2 Standard TTCP models (One model with wrap-around fins and the other model with flat fins)	Computational	0.5-2.0	1.5
K. Ravi, et.al. [9]	Standard TTCP with pinched and blunt leading edge	Numerical and computational study	1.2-2.5	1.2-1.4
C. M. Thomas, et.al. [10]	Two finned model (one is solid fin and other is slotted model)	Flight experiment tests	2.15-3.83	-
A. Gregg [11]	WAF model	Computational	0.4-3.5	1

2. NUMERICAL FORMULATION

Computational fluid dynamics or CFD analysis is a vital analysis involving the heat transfer, fluid flows, and various phenomena through computational simulations used in engineering applications.

Conservation of mass, conservation of momentum, conservation of energy are the three fundamental principles with which the physical aspects of CFD are governed. These principles are expressed in partial differential equations to obtain a numerical description of the flow field.

Continuity equation:

$$\frac{\partial \rho}{\partial t} + \nabla \cdot (\rho \mathbf{V}) = 0 \tag{1}$$

Momentum equation:

$$\rho \frac{\mathrm{Dv}}{\mathrm{Dt}} = \nabla \boldsymbol{\tau}_{\mathrm{ij}} - \nabla \mathbf{p} + \rho \mathrm{F} \tag{2}$$

Energy equation:

$$\rho \frac{\mathrm{D}e}{\mathrm{D}t} + \rho(\nabla \cdot \mathbf{V}) = \frac{\partial Q}{\partial t} - \boldsymbol{\nabla} \cdot q + \varphi \tag{3}$$

The Euler equation in strong conservative form is used to describe the mean flow property of the field.

From the given above governing equations, the Euler equation is developed by considering inviscid and adiabatic (i.e., flow having a zero thermal conductivity and a zero viscosity) as flow conditions.

The Euler equations can be applied for both compressible and incompressible flow. It is expressed as,

$$\frac{\partial \boldsymbol{\omega}}{\partial t} + \frac{\partial \boldsymbol{F}_x}{\partial x} + \frac{\partial \boldsymbol{F}_y}{\partial y} + \frac{\partial \boldsymbol{F}_z}{\partial z} + \boldsymbol{G} = 0 \tag{4}$$

where,

$$\boldsymbol{\omega} = \begin{pmatrix} \rho \\ \rho u_1 \\ \rho u_2 \\ \rho u_3 \\ E \end{pmatrix}, \boldsymbol{G} = \begin{pmatrix} 0 \\ -f_x \\ -f_y \\ -f_z \\ 0 \end{pmatrix}$$

$$\boldsymbol{F}_x = \begin{pmatrix} \rho u_1 \\ \rho u_1^2 + \mathrm{P} \\ \rho u_1 u_2 \\ \rho u_1 u_3 \\ u_1(\mathrm{E} + \mathrm{P}) \end{pmatrix}, \boldsymbol{F}_y = \begin{pmatrix} \rho u_2 \\ \rho u_1 u_2 \\ \rho u_2^2 + \mathrm{P} \\ \rho u_2 u_3 \\ u_2(\mathrm{E} + \mathrm{P}) \end{pmatrix}, \boldsymbol{F}_z = \begin{pmatrix} \rho u_3 \\ \rho u_1 u_3 \\ \rho u_2 u_3 \\ \rho u_3^2 + \mathrm{P} \\ u_3(\mathrm{E} + \mathrm{P}) \end{pmatrix}$$

The flow variable vector is **ω** and the flux vectors are $\boldsymbol{F}_x$, $\boldsymbol{F}_y$, $\boldsymbol{F}_z$. u_1, u_2, u_3 are the velocity components in x, y, z directions, respectively. E is the total specific internal energy; P is the pressure; ρ is the density of flow.

3. COMPUTATIONAL ANALYSIS

The Technical Cooperation Program (TTCP) has developed the basic configuration of the standard wraparound fin projectile. The standard TTCP model is modified to develop the three models. Four models have been designed in SolidWorks software using the part mode and the assembly mode. The models are:

i. Standard TTCP (with 45° Leading Edge)
ii. Standard TTCP with Blunt Leading Edge
iii. Standard TTCP with Blunt Leading Edge and 30° Sweep
iv. Standard TTCP with 45° Leading Edge and 30° Sweep

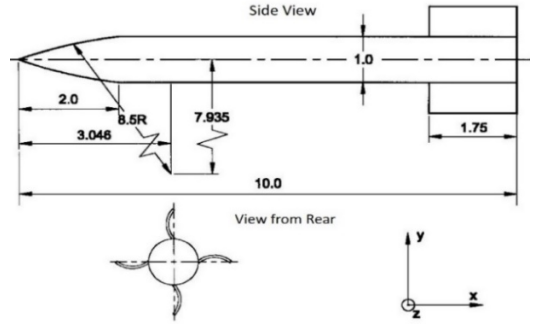

Figure 1: Standard TTCP model geometry [4]

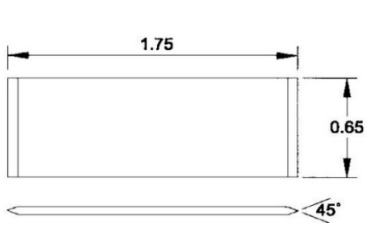

Figure 2: Standard TTCP model fin geometry [4]

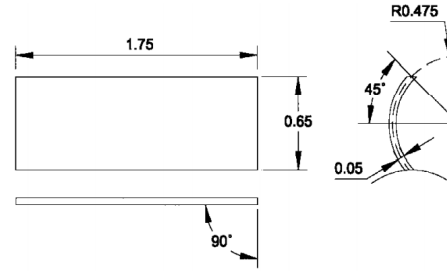

Figure 3: Standard TTCP model fin geometry having blunt leading edge [4]

The meshing of the solid models was performed using the 'Pointwise' pre-processing software. The particular type of grid used in meshing the project is the voxelgrid, a type of unstructured grid. The wall y^+ value for near body boundary refinement is considered to be less than 1. The boundary conditions that were used for the computation are a wall for the model, pressure far-field inlet and pressure outlet for the external far-field domain inlet and outlet, respectively.

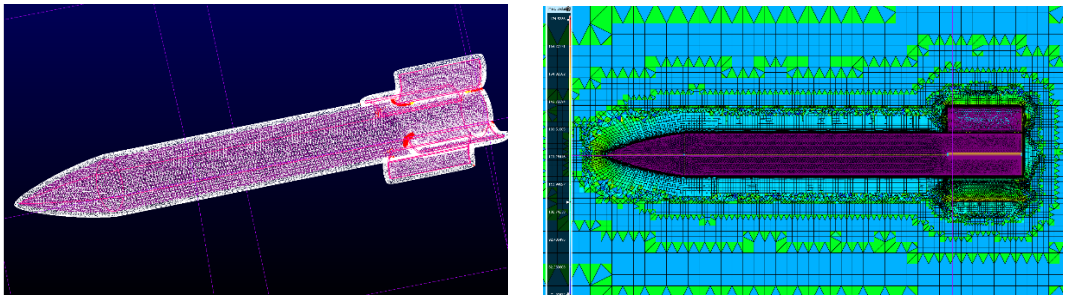

(a) (b)

Figure 4: TTCP Standard model mesh in pointwise (a) Boundary layer generation, (b) Near body refinement of a mesh

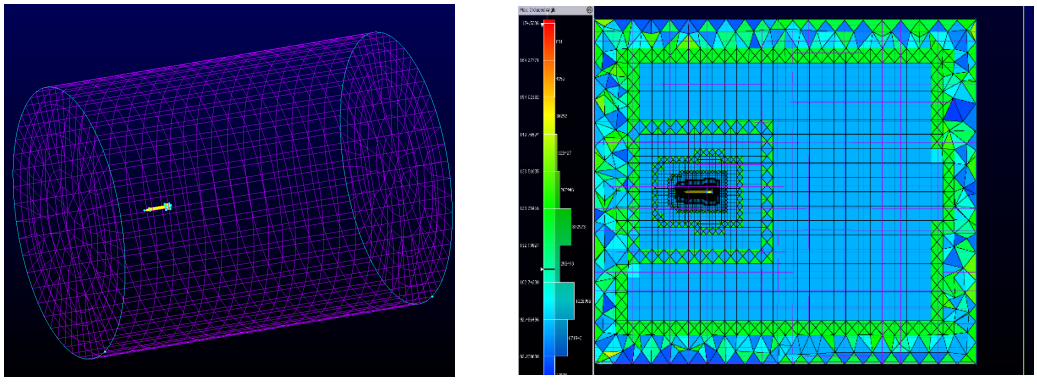

(a) (b)

Figure 5: (a)An external far-field domain, (b)The volumetric mesh of far-field domain

The model is then exported to the ANSYS FLUENT solver to obtain the solution. Since the solvers use different numeric and primitive variables, they generate different results. A density-based solver with an implicit approach is best suitable for this model analysis, for which the Mach number ranges from 1.5 to 2.5. The effect of coefficient of rolling moment was analysed using a modified k-epsilon turbulence model (Realizable). An ideal gas was considered as the material type in the flow for analysis. The property of the ideal gas for analysis was based on the Sutherland's law. The Courant number ranges between 0.15 and 0.5 from the first order and second order solutions, to attain stability and convergence. In FLUENT post-processing, the residual plot and the mass flow rate showed the convergence of the solution.

4. RESULTS AND DISCUSSIONS

Staying open and responsive to unexpected trends, gestures, and outcomes are one of the most important things researchers are supposed to do when analysing data. The solution obtained in ANSYS FLUENT was compared with the previous research works to check the solution accuracy. Figure-6 shows the comparison of the present result with experimental and computational data obtained by Edge [6], Dalkhe [2], Paek [4] as a function of Mach number, roll moment coefficient. It indicates that the cross-over point is around the Mach number 1.8, i.e., the rolling moment coefficient at that point is zero. The trend of the curve of our result is similar to that of previous research works. Hence, the same methodology was used and studied for the other three models.

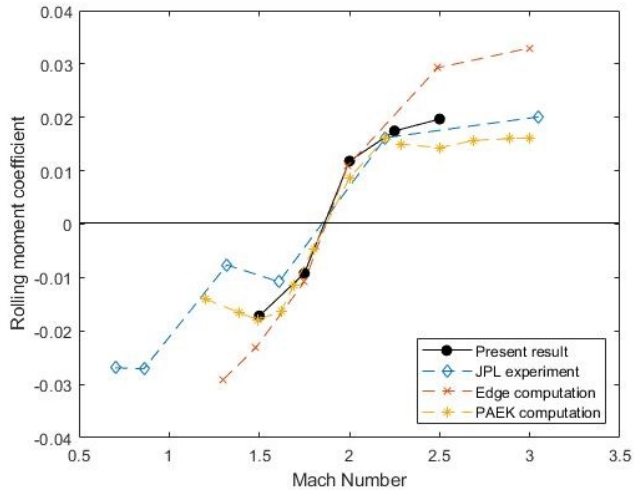

Figure 6: Data comparison of our work with previous computational and experimental work

The results of static pressure contours on the surface of convex and concave sides for all TTCP Standard and TTCP Standard modified wrap-around fin models at Mach 2.0 were represented. To observe the pressure distribution after the point at which the rolling moment coefficient is zero, the Mach number (M=2.0) is selected. The solution of the rolling moment from Mach number 2.0 is observed to be positive. Due to the formation of expansion and compression shocks from the fin's leading edge, the pressure distribution on the rear end of the adjacent fin is affected.

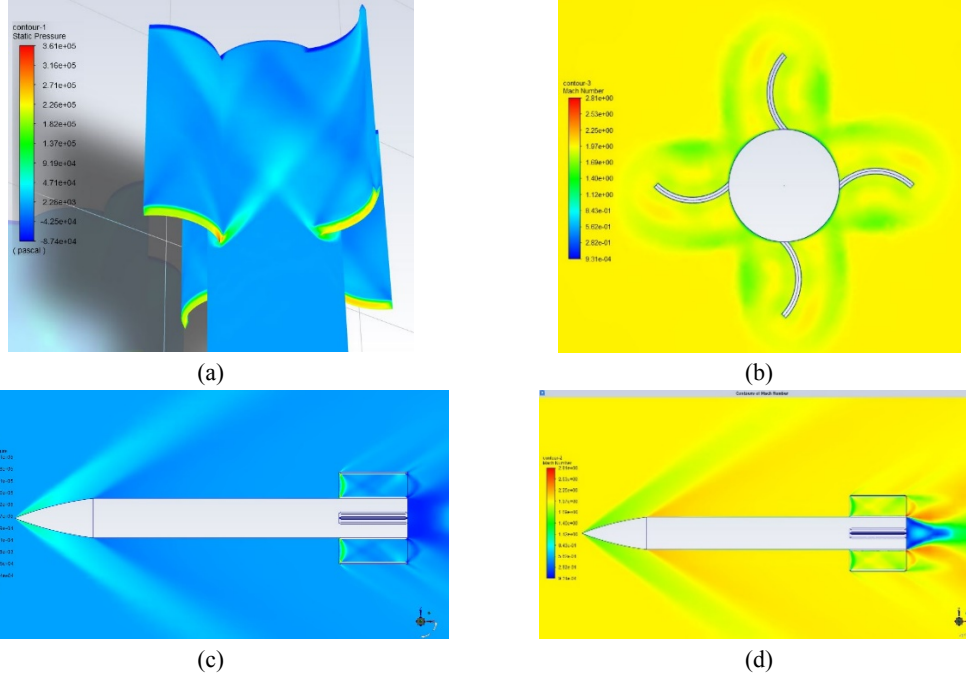

(a) (b)

(c) (d)

Figure 7: Standard TTCP with 45° leading-edge; (a) Surface static Pressure contour of wrap-around fins, (b)A rear view of Mach number variation of the far-field domain around the wrap-around fins, (c) Static Pressure contour of the far-field domain around the model, (d)Mach number variation of the far-field domain around the model

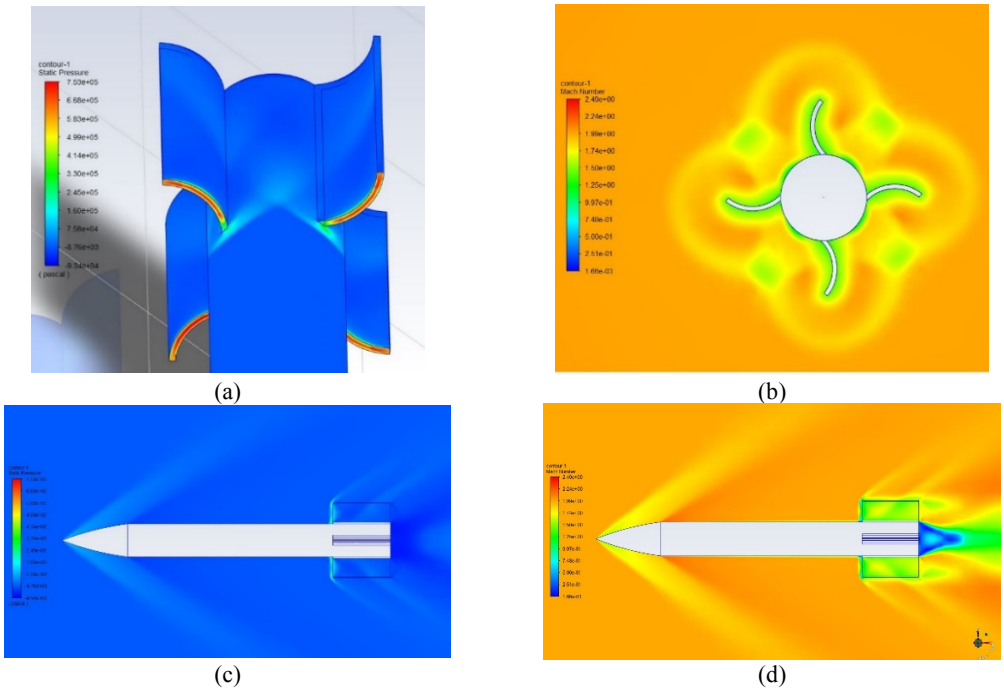

(a) (b)

(c) (d)

Figure 8: Standard TTCP with blunt leading-edge; (a) Surface of static Pressure contour of wrap-around fins, (b)Rear view of Mach number variation of the far-field domain around the wrap-around fins, (c)Static Pressure contour of the far-field domain around the model, (d)Mach number variation of the far-field domain around the model

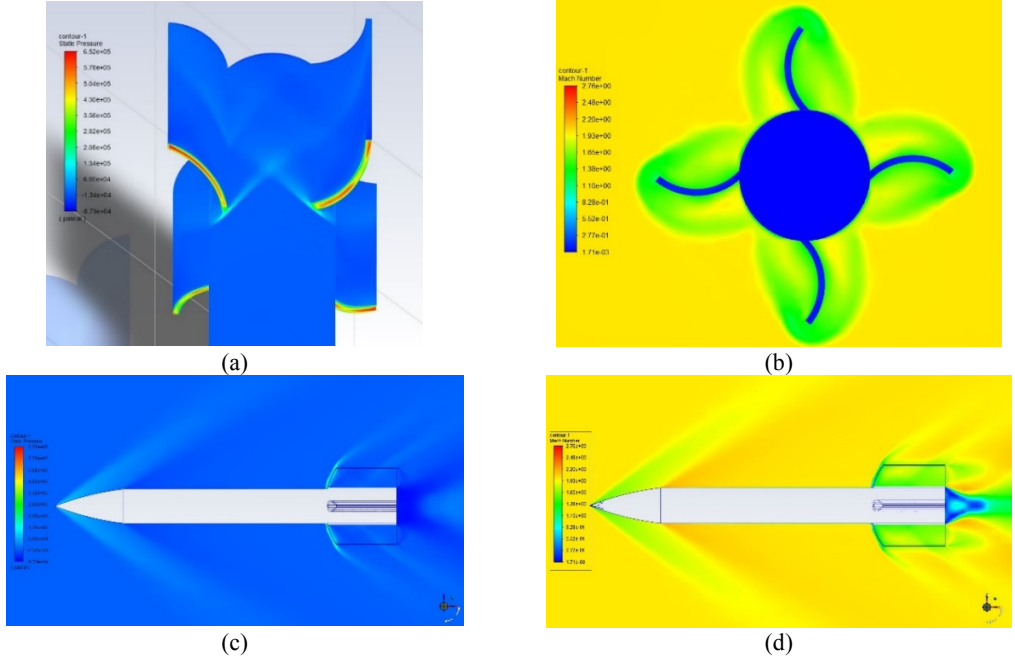

(a) (b)

(c) (d)

Figure 9: Standard TTCP with blunt leading-edge and 30° sweep; (a)Surface of static Pressure contour of wrap-around fins, (b)Rear view of Mach number variation of the far-field domain around the wrap-around fins, (c)Static Pressure contour of the far-field domain around the model, (d)Mach number variation of the far-field domain around the model

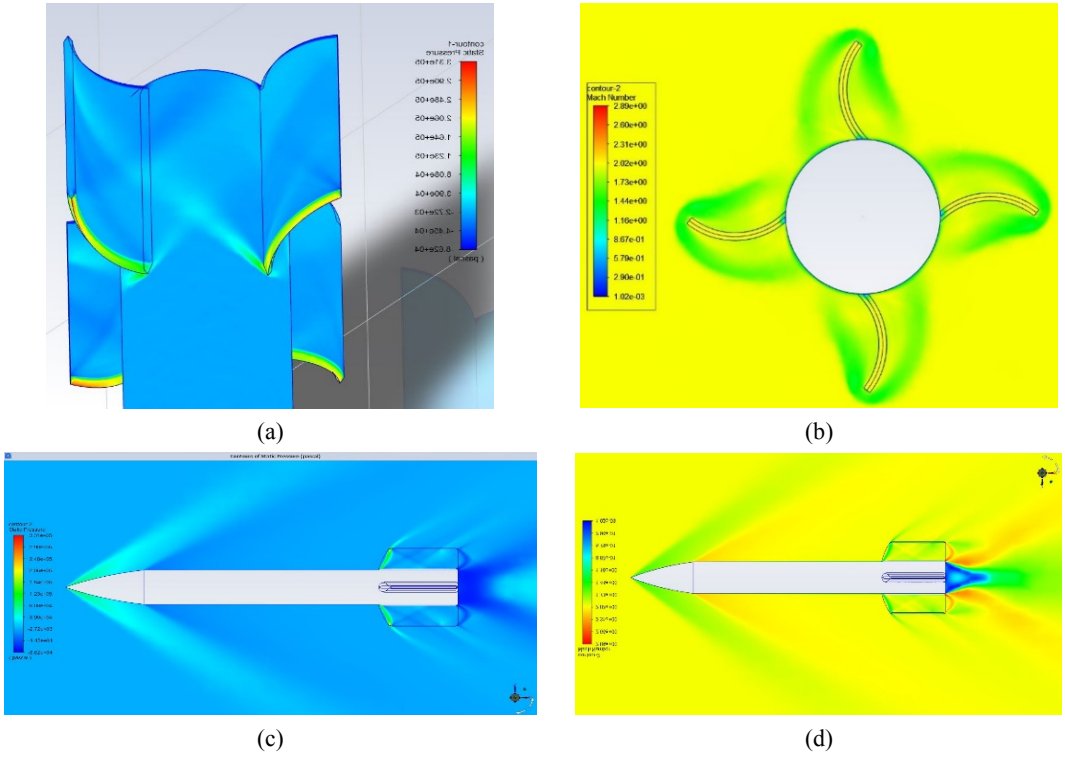

Figure 10: Standard TTCP with 45° leading-edge and 30° sweep; (a)Surface of static Pressure contour of wrap-around fins, (b)Rear view of Mach number variation of the far-field domain around the wrap-around fins, (c)Static Pressure contour of the far-field domain around the model, (d)Mach number variation of the far-field domain around the model

As the solutions converge, the co-efficient of drag and coefficient of the rolling moment are obtained for a Mach number ranging from 1.5 to 2.5 with the interval of 0.25 for the entire four models.

Figure-11 describes the comparison of all the four models plotting the rolling moment coefficient as a function of Mach number in a lower supersonic region ranging from 1.5 to 2.5 in the interval of 0.25, to study the effect of leading-edge sweep.

The roll reversal of the wrap-around design for the standard TTCP model generally occurred around the Mach number 1.8. Since there is an effect of compression and expansion waves, the roll reversal is delayed towards a higher Mach number.

For the blunt leading edge, the roll reversal occurred in a lower supersonic region of the Mach number 1.6. In contrast, for the TTCP model having a blunt leading edge with a 30° sweep, the roll reversal occurred at two points, i.e., around M=1.7 and M=1.8.

The blunt leading-edge model with a 30° sweep has a positive rolling moment in the lower supersonic speed.

As the Mach number increases, the positive rolling moment coefficient changes to negative, resulting in a roll reversal, and then it follows a similar pattern as the TTCP standard model.

The standard TTCP model with a 45° leading edge and the 30° sweep follow a similar path to the standard TTCP model with 45° leading edge. However, they differ in the magnitude of the rolling moment coefficient.

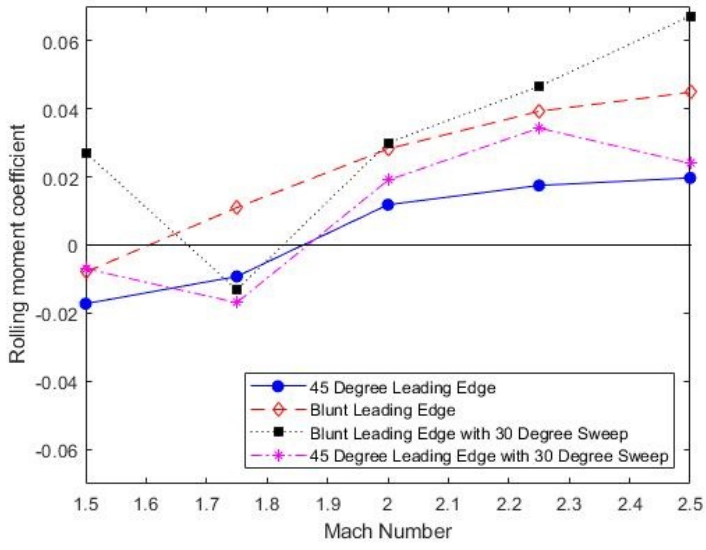

Figure 11: Comparison graph of four modified models of TTCP

5. CONCLUSIONS

The general roll characteristics for wrap-around fins were analysed in the supersonic region, where Mach is in the range from M=1.5 to M=2.5. By evaluating Navier-Stokes equations, flow field solutions were generated for WAF. Grids were uniformly dispersed around the flow field of a TTCP model, both near the nose tip and near the fin edge. From the flow field solutions, the roll moment coefficients were estimated and compared to experimental results. With reference to magnitude and signs, the computed roll moment coefficients for the standard TTCP model were in reasonable agreement with the numerical findings.

The formation of expansion and compression waves from the tip of fin due to the effect of flow from adjacent fin is observed for all the models and for, blunt leading edge this effect is more compared with the 45° leading-edge TTCP model. It is observed that the sweep angle and the tip geometry of the fin have a significant effect on the rolling moment for the missile.

6. FUTURE WORK AND APPLICATIONS

Wrap-around fin configuration is deliberately useful for the missiles due to its high packing factor capacity. It is also very convenient in terms of storage as it occupies an inconsiderable amount of space in the missile geometry.

As presented in the report, the simulations and analysis have only been done to zero angle of attack. Keeping in the mind the future tasks, this analysis can be carried out further by performing the research at a various angle of attack and comparing the results with the above analysis to determine the behaviour of roll reversal and roll moment on the fins at various operating conditions. The effect of leading-edge sweep and leading-edge angle can be collated at numerous ranges and the best values can be rolled out for the production of wrap-around fin configured missiles, which gives exceptional performance and reliability.

ACKNOWLEDGEMENT

This project work was supported/partially supported by Bharat Dynamics Limited, Hyderabad and Institute of Aeronautical engineering, Hyderabad. We are grateful to the Dr. D Govardhan, Head of the Aeronautical Engineering Department, IARE and Dr. L V Narsimha Prasad, Principal, IARE for providing us with all the resources in the college to make our project a success.

We thank Mr. Manikandan D (Assistant Manager, D&E) for contributing to the 3D modelling of Standard TTCP having 45° leading-edge and 30° sweep solid model. We would also like to extend our thanks to D&E support staff as well as all other departments that contributed directly or indirectly to the success of this project.

REFERENCES

[1] C. W. Dahike, *The Aerodynamic Characteristics of Wrap-Around Fins at Mach Numbers of 0.3 to 3.0*, U.S. Army Missile Command, TR RD-77-4, Alabama, 1976.

[2] C. Dahlke, *The effect of wrap-around fins on aerodynamic stability and rolling moment variations*, Army Missile Command Redstone Arsenal, Alabama, 1973.

[3] S. Arnan and B.-H. Benjamin, *The Evaluation of the Rolling Moments Induced by Wraparound Fins*, National Aeronautics and Space Administration, California, 1983.

[4] P. Seung-Kil Paek, P. Tae-Sang, B. Jae-Sung, L. In and H. K. Jang, Computation of Roll Moment for Projectile with Wraparound Fins Using Euler Equation, *Journal of Spacecraft and Rockets,* Vols. **36**, No.1, pp. 53-58, 1999.

[5] M. Slobodan, Analysis of the Rolling Moment Coefficients of a Rockets with Wraparound Fins, *Scientific-Technica ,* vol. **2**, no. Review, pp. 30-37, 2006.

[6] H. L. Edge, Computation of the Roll Moment for a Projectile with wrap-around fins, *Journal of Spacecraft and Rockets,* Vols. **31**, No. 4, p. 615–620, 1994.

[7] Y. K. Jung, C. Sung-In, In-Lee, N. Hyoung-Jin and J. Sang-Young, Aerodynamic Analysis of a Rolling Wraparound Fin Projectile in Supersonic Flow, in *International Journal of Modern Physics*, Korea, 2012.

[8] L. W. Brett, *Aerodynamics of Wraparound Fins in Supersonic Flow*, Redstone Arsenal, AL 35898 , 2006.

[9] K. Ravi, S. Rhishabh, K. Abhijit and G. A. K., Anomalies in the Flow over Projectile with Wrap-around Fins, *Defence Science Journal,* Vols. **59**, No. 5, pp. 471-484, 2009.

[10] C. M. Thomas, D. B. Rodney and P. G. Larry, "Effects of Mach number on supersonic Wraparound Fin aerodynamics," *Journal of Spacecraft and Rockets,* vol. **35**, no. 6, pp. 742-748, 1998.

[11] A. Gregg and C. Theresa, Analysis of missile configurations with wrap-around fins using computational fluid dynamics, *Flight Simulation and Technologies,* 1993.